

# Evaluation of magnetic poly(methyl methacrylate) microspheres as catalysts in heterogeneous Fenton processes

Alan Kardec da Silva<sup>1</sup> , Ezaine Cristina Corrêa Torquato<sup>1</sup> , Jacira Aparecida Castanharo<sup>2</sup> , Marcos Antonio da Silva Costa<sup>2</sup> , Mônica Regina da Costa Marques<sup>3</sup> and Luciana da Cunha Costa<sup>1\*</sup>

<sup>1</sup>Departamento de Farmácia, Faculdade de Ciências Biológicas e da Saúde, Campus Zona Oeste, Universidade do Estado do Rio de Janeiro – UERJ, Rio de Janeiro, RJ, Brasil

<sup>2</sup>Departamento de Processos Químicos, Instituto de Química, Universidade do Estado do Rio de Janeiro – UERJ, Rio de Janeiro, RJ, Brasil

<sup>3</sup>Departamento de Química Orgânica, Instituto de Química, Universidade do Estado do Rio de Janeiro – UERJ, Rio de Janeiro, RJ, Brasil

\*luciana.cunha.costa@gmail.com

## Abstract

This work reports the preparation of magnetic polymeric microspheres based on poly(methyl methacrylate) and the investigation of these materials as catalysts in heterogeneous Fenton processes for the decolorization of methyl orange (MO). The microspheres were prepared by polymerization of the magnetic material together with the monomers by aqueous suspension polymerization. The microspheres had specific surface area of  $48.2\text{ m}^2\text{ g}^{-1}$ . Mossbauer data indicated that the magnetic material was a mixture of magnetite (31%), maghemite (21%), and goethite (48%). Fenton reactions were performed by varying the concentration of  $\text{H}_2\text{O}_2$ , pH, composite mass, and contact time. The highest color removal rates (around 80%) were reached at pH 3.0, 20% w/v of composite, 20 minutes contact time, and 10 ppm of  $\text{H}_2\text{O}_2$ . The composite could be reused during four cycles with removal efficiency above 50%. The results indicated that the adsorption and oxidation mechanisms act together determining the variation of the MO dye removal.

**Keywords:** heterogeneous Fenton reactions, magnetic materials, methyl orange, poly(methyl methacrylate) microspheres.

**How to cite:** Silva, A. K., Torquato, E. C. C., Castanharo, J. A., Costa, M. A. S., Marques, M. R. C., & Costa, L. C. (2022). Evaluation of magnetic poly(methyl methacrylate) microspheres as catalysts in heterogeneous Fenton processes. *Polímeros: Ciência e Tecnologia*, 32(2), e2022018. <https://doi.org/10.1590/0104-1428.20220029>

## 1. Introduction

Synthetic organic dyes, especially azo dyes, are employed in various industrial processes where byproducts are these contaminants; consequently, these dyes are released in the wastewater of these industries<sup>[1,2]</sup>. According to Tunç et al.<sup>[3]</sup>, “these pollutants absorb and reflect the sunlight entering the water and hence hinder the photosynthesis in aquatic plants.” These pollutants are toxic to the environment, especially aquatic lives, and conventional treatment processes for their removal are often inefficient due to their high stability and complex nature<sup>[1-4]</sup>.

The Fenton process is highlighted among several advanced oxidation processes (AOPs) due to its simple operation, low cost, low toxicity of the reactants, and ability to treat many hazardous organic contaminants. Fenton’s reagent is a mixture of  $\text{H}_2\text{O}_2$  and  $\text{Fe}^{2+}$  or  $\text{Fe}^{3+}$  ions (in stoichiometric amounts), generating OH and OOH radicals, at acid pH<sup>[3]</sup>. The replacement of homogenous Fenton catalysts by heterogeneous approaches has been motived by considering the straightforward recovery, possible recycling, or reuse of these heterogeneous materials, and reduction of the amount

of Fe leached into the medium, besides the possibility of expanding the pH range of using these materials<sup>[5]</sup>.

Magnetic composites have received considerable attention due to their easy separation from the medium. These composites can be used in many areas, such as catalysis, environmental remediation, and biomedical processes<sup>[6-8]</sup>. A search of a scientific research platform employing the keywords “magnetic composites and heterogeneous Fenton” showed an increase in the number of publications over the years (Figure S1 – Supplementary Material). Several magnetic composites based on polymers have been studied as heterogeneous Fenton and Fenton-like catalysts and evaluated for dye degradation. The polymers used in the preparation of these composites can be carbon-based polymers such as carbon nanotubes<sup>[1,9]</sup>, carbon nanofibers<sup>[9]</sup>, graphene and graphene oxide<sup>[2,9,10]</sup> and biopolymer matrices such as alginate<sup>[11]</sup>.

According to Gao et al.<sup>[12]</sup>, polymeric microspheres based on poly (methyl methacrylate) (PMMA) stand out among other types of microspheres (polystyrene, poly (ethylene glycol),

poly(glycidyl methacrylate), etc), due to the properties of PMMA, such as high impact strength, light transmissivity, good processability, and biocompatibility. These microspheres can be prepared by various polymerization techniques and functionalized through different strategies. The preparation of composites from PMMA microspheres can contribute to increasing the “chemical stability, mechanical strength, catalytic performance” of these materials. The synergism between the properties of these polymers and magnetic materials can enable the preparation of materials with superior properties<sup>[8]</sup>. However, no studies reported the evaluation of these microspheres as catalysts in heterogeneous Fenton processes. Shan et al.<sup>[13]</sup> report the preparation of magnetic porous Fe<sub>3</sub>O<sub>4</sub>/poly(methyl methacrylate-co-divinylbenzene) microspheres and their use as adsorbent of Rhodamine B dye. However, the authors did not study the employment of this material as a catalyst in a Fenton process and the relationship between the reaction conditions and the efficiency of this catalyst.

Because magnetic polymeric microspheres based on PMMA have not been sufficiently studied as catalysts of heterogeneous Fenton processes, this work describes the preparation of magnetic polymeric microspheres based on PMMA and the investigation of these materials as catalysts in heterogeneous Fenton processes for the decolorization of methyl orange (MO). The influence of the experimental conditions (pH, contact time, mass of composite, H<sub>2</sub>O<sub>2</sub> concentration) on the discoloration rate of the dye solutions was investigated. The lifetime of the catalysts was also analyzed in ten cycles of reuse. The azo dye methyl orange (MO) was chosen as the target organic pollutant due to its low cost, wide application, and stability<sup>[1,4,11,14]</sup>

## 2. Materials and Methods

### 2.1 Preparation of magnetic material

The synthesis of magnetic material was performed by the co-precipitation technique. Initially, 27 g of FeCl<sub>3</sub> and 14 g of FeSO<sub>4</sub>·7H<sub>2</sub>O were solubilized in deionized water (50 mL).

These solutions were transferred to 250 mL three-necked round-bottomed reactor flask equipped with a mechanical stirrer and maintained under stirring (150 rpm) in a nitrogen atmosphere until complete dissolution of the reactants. Then 130 mL of NH<sub>4</sub>OH (28% NH<sub>3</sub> in H<sub>2</sub>O) was slowly added to the reactor. The solution was maintained under stirring at 70 °C for 1 h. The result of this step was a black residue. It was washed several times with deionized water until the supernatant pH was around 7. Subsequently, under gentle stirring at a temperature of 80 °C, 10 mL of oleic acid was added. The reaction lasted 30 minutes. The final mixture was washed with ethanol several times to remove excess oleic acid and was transferred to a desiccator. The air was evacuated and replaced by nitrogen for each use<sup>[6,7]</sup>. Inorganic reactants were acquired from Vetec Química Ltda. Oleic acid was acquired from B. Herzog Varejo de Produtos Químicos Ltda. All reactants were used as received.

### 2.2 Preparation of magnetic PPMA microspheres

Magnetic polymeric microspheres were prepared by aqueous suspension polymerization in a 1 L reactor flask

equipped with a mechanical stirrer and a reflux condenser containing a silicon oil seal at the top. The organic phase was composed of 90 wt. % of methyl methacrylate (MMA), 10 wt.% of divinylbenzene (DVB), n-heptane (100% to the volume of monomers), 2,2-azobisisobutyronitrile (AIBN) (2% wt.% to monomers), and of magnetic material (5 wt. % to monomers). This mixture was left in a thermostatic bath at 50 °C for 30 min under stirring (150 rpm). The aqueous phase consisted of 1 wt.% of poly(vinyl alcohol) (PVA) to water volume, 1 wt.% of NaCl to water volume, and distilled water. The volumetric ratio between the aqueous and organic phases was 4:1. The aqueous phase was transferred to the reactor flask, and the stirring was set to 700 rpm. Then the organic phase was dropwise transferred to the reactor. The reaction was maintained under stirring at 80 °C for 4 h<sup>[6]</sup>. The final product was washed extensively with heated deionized water and dried at 60 °C. AIBN was acquired from Mig Química and used after recrystallization with methanol. The monomers were donated by Lanxess Ltda and Nitriflex Ltda respectively. PVA was donated by Kurary Inc. Other reactants were acquired from Vetec Química Fina. These reactants were used as received.

### 2.3 Characterization of polymeric microspheres

The magnetic microspheres were characterized by optical microscopy (Olympus BX51M), scanning electron microscopy together with energy-dispersive X-ray spectroscopy (SEM-EDS) (Fei Inspect 550), vibrating sample magnetometry (VSM) (Lake Shore 7400), Mössbauer spectroscopy (Fast Comtech, Germany), particle size distribution (Malvern Mastersizer 2000), specific surface area, pore volume, and pore diameter by employing nitrogen physisorption (Micromeritics ASAP 2020 apparatus). The sample's crystalline structure was verified by X-ray diffractometry (Shimadzu, model XRD 6000). Scans were performed between 7-70° (2θ) with a goniometer speed of 2° per minute. The JADE program was used to identify mineralogical phases present in the samples. For SEM-EDS analysis, the samples were metalized with gold, and an acceleration voltage of 15 kV and magnification of 250 x was used. Specific surface area, pore volume and pore diameter were determined by employing BET and BJH Equations. Mossbauer spectroscopy was used to identify the magnetic material according to the method described by Castanharo et al.<sup>[6,7]</sup>. The FT-IR spectra of all polymers were recorded with a Perkin-Elmer Spectrum One spectrometer, (4000-400 cm<sup>-1</sup>, 4 scans, and 4 cm<sup>-1</sup> resolution) in the form of KBr discs. The content of iron incorporated in the particles was determined by AAS spectroscopy after digestion of the microspheres by employing HNO<sub>3</sub>:HCl 1:3 v/v according to the method previously published<sup>[6]</sup>.

### 2.4 Heterogeneous Fenton tests employing magnetic microspheres for dye decolorization

Decomposition tests of methyl orange were conducted using a batch system in Erlenmeyer flasks (250 mL) on stirring plates under slow agitation. The tests were performed by varying the mass of magnetic microspheres (1-20% w/v), the concentration of H<sub>2</sub>O<sub>2</sub> (0.1-50 ppm), pH of the medium, adjusted with acetic acid/acetate buffer 0.5 mol L<sup>-1</sup> (3.0-7.5), and contact time between the solution and microspheres (0 – 30 min). The final volume of the medium was maintained

at 100 mL, while the dye concentration was 5 ppm, and the reaction temperature was 25 °C. Considering the possibility of dye adsorption by the composite, we also performed tests in the absence of H<sub>2</sub>O<sub>2</sub>, employing composite concentrations of 5, 10, or 20% w/t% (in relation to the total volume of the medium), pH 3.0, and 10 minutes of contact between the microspheres and dye solution. Aliquots of 5 mL of the supernatant collected after the reaction were transferred to a quartz cuvette and read at 500 nm. All experiments were conducted in duplicate, and the results are presented as average. Efficiency in removing MO was calculated by using Equation 1<sup>[15]</sup>.

$$R(\%) = \frac{(C_0 - C_t)}{C_0} \times 100 \quad (1)$$

where: R (%) is removal efficiency (%), C<sub>0</sub> is initial MO concentration (mg/L), and C<sub>t</sub> is MO concentration at time t (mg/L).

The studies of reuse of the microspheres as catalysts were conducted in ten batch cycles employing 5% w/v of catalyst, 5 ppm of H<sub>2</sub>O<sub>2</sub>, 5 ppm of dye, pH 3.0, and a final medium volume of 10 mL. After each reuse cycle, the microspheres were separated from the reaction medium by filtration, rinsed with distilled water, and placed in another Erlenmeyer for a new experiment. After each cycle, the dye decomposition was evaluated by collecting 5 mL samples of the supernatant and analyzing them at 500 nm with a spectrophotometer (Shimadzu, model UV-VIS – 1240).

### 3. Results and Discussion

Magnetic polymeric particles were prepared by polymerizing magnetic material with the monomers MMA and DVB by aqueous suspension polymerization. SEM images shows showed these particles' spherical shapes (Figure 1a). Malvern data showed that these particles had large size distribution (Table 1). EDS spectra indicated the presence of Au metal (used in the coating of particles for

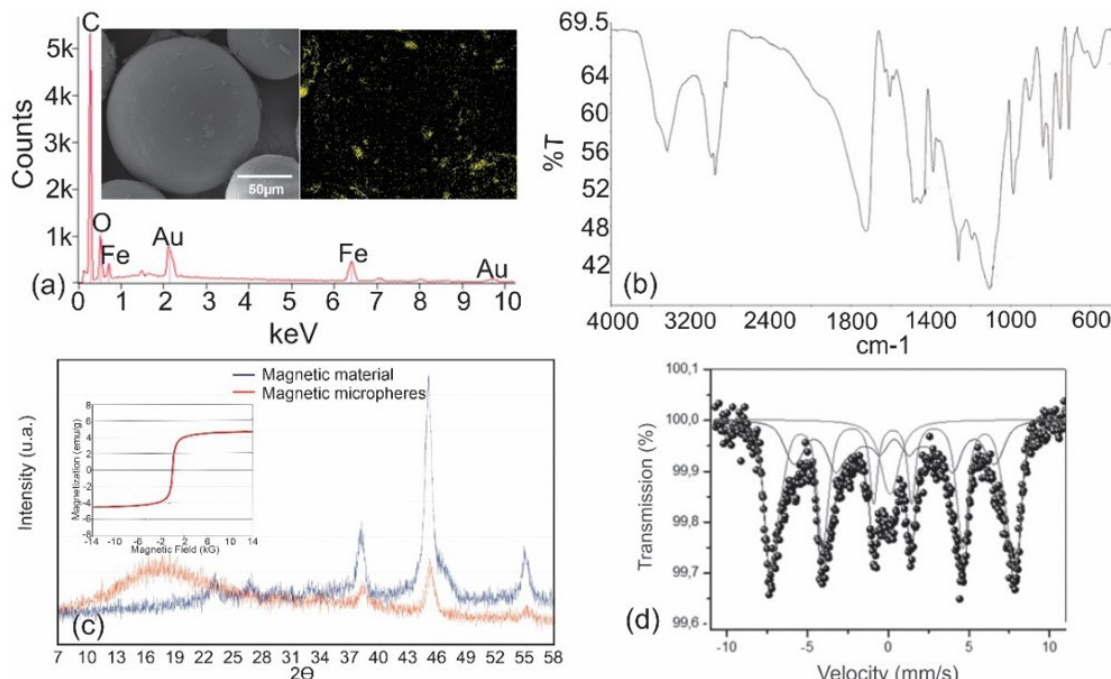


**Figure 1.** (a) EDS spectrum and iron distribution map of the magnetic material, SEM image of magnetic microsphere; (b) FT-IR spectrum of the magnetic microspheres; (c) XRD spectra of the magnetic material and magnetic microspheres; (d) Transmission Mossbauer spectra of the magnetic microspheres.

**Table 1.** Morphological characteristics of the magnetic PMMA microspheres<sup>[6]</sup>.

S (m <sup>2</sup> g <sup>-1</sup> )	V <sub>p</sub> (cm <sup>3</sup> g <sup>-1</sup> )	P. S.(μm)	M <sub>s</sub> (emu g <sup>-1</sup> )	M <sub>R</sub> (emu g <sup>-1</sup> )	I.C. (% m.m.)
48.30	0.35	20-104.00	4.76	0.21	4.13 ± 0.02

S: specific surface area (determined by nitrogen physisorption, by employing the BET equation); V<sub>p</sub>: pore volume (determined by nitrogen physisorption, by employing the BJH equation); P.S.: Particle size range (determined by Malvern Mastersizer), M<sub>s</sub>: saturation magnetization (determined by employing vibrating sample magnetometry), M<sub>R</sub>: remaining magnetization (determined by employing vibrating sample magnetometry), I.C.: iron content incorporated in the polymeric particles (determined by AAS after acid digestion of the particles)

SEM analysis); besides Fe, confirming the incorporation of the magnetic material on microspheres, along with carbon and oxygen, due to polymeric matrix composed of DVB and MMA (Figure 1a). The Fe distribution map of magnetic material (obtained through the EDS accessory) (Figure 1a) showed small yellow dots (Fe domains) distributed over the entire surface of the polymeric microspheres, along with yellow clusters, indicating that magnetic material was heterogeneously incorporated in the polymeric matrix. FT-IR spectrum of magnetic microspheres (Figure 1b) showed bands at  $1724\text{ cm}^{-1}$  due to stretching of the C=O bond of the ester group,  $1605\text{ cm}^{-1}$  due to C=C stretching of the aromatic ring,  $1461\text{ cm}^{-1}$ , and  $1388\text{ cm}^{-1}$  due to asymmetric and symmetric stretching of the O-CH<sub>3</sub> bond of the ester group,  $1261\text{ cm}^{-1}$ , and  $1107\text{ cm}^{-1}$  related to coupled asymmetric stretching C(=O)-O and O-C-C, besides a band at  $3438\text{ cm}^{-1}$  due to hydrogen bonding between carbonyl and oxygen of the (moist) MMA ester and water<sup>[16]</sup>.

Peaks related to iron oxides were identified in the positions  $22.9^\circ$ ,  $38.0^\circ$ ,  $45^\circ$ ,  $54.9^\circ$ , and  $68.7^\circ$  ( $2\theta$  plane),  $472^\circ$ ,  $270^\circ$ ,  $333^\circ$ ,  $175^\circ$ , and  $90^\circ$  (crystalline plane), in the diffractograms produced by XRD analysis of magnetic material and magnetic microspheres (Figure 1c). It was also possible to observe peaks due to goethite at  $28^\circ$  and  $41^\circ$ . XRD spectra of the magnetic material and magnetic microspheres showed the same peaks related to iron oxides, indicating that the structure of the magnetic material was preserved during polymerization<sup>[6,7]</sup>. However, it was also possible to observe the presence of an amorphous halo in the diffractogram of the magnetic microspheres, related to the polymeric matrix of this material. Magnetic microspheres presented saturation magnetization ( $M_s$ ) of  $4.76\text{ emu g}^{-1}$  and remnant magnetization ( $M_r$ ) of  $0.21\text{ emu g}^{-1}$ , indicating a good response to the magnetic field and superparamagnetic behavior (Table 1). The magnetization curve did not have a hysteresis loop (Figure 1c), confirming this superparamagnetic behavior.

Mössbauer spectra of these magnetic polymers (Figure 1d) showed a contribution from a doublet, indicating the presence of superparamagnetic particles, and an asymmetric sextet, added to the pure magnetic material, but with a slight loss of intensity of the magnetic transmission. This result also indicates that the polymerization did not change the properties of the magnetic particles. However, the polymerization may cause a change in the inter-particle interaction parameters, making qualitative interpretation and theoretical calculation of these polymer composites' spectra difficult<sup>[17]</sup>. The interparticle interactions were mainly: (i) dipole-dipole interaction and (ii) exchange interaction through the surface of the particles. In the case of magnetic polymers, the second interaction can be neglected because the dipolar interaction dominates the interparticle interaction<sup>[18]</sup>. This interparticle interaction can explain the difference between magnetic transmission on pure magnetic material and magnetic polymers. Mössbauer results also indicated that the magnetic material is a mixture of magnetite ( $\text{Fe}_3\text{O}_4$ , 31%) and maghemite ( $\gamma\text{-Fe}_2\text{O}_3$ , 21%), minerals with magnetic behavior, agreeing with the data on  $M_s$  and  $M_r$ , and goethite ( $\alpha\text{-FeOOH}$ , 48%). Part of the magnetite was converted into maghemite by partial oxidation of  $\text{Fe}^{2+}$  to  $\text{Fe}^{3+}$  and magnetic particles containing a low concentration of  $\text{Fe}^{2+}$  ions.

The microspheres had large specific surface area and pore volume, even though containing magnetic material in their structure (Table 1). The content of iron incorporated in the polymer (determined by AAS before acid digestion of the particles) was 4.76 wt.%, indicating a high degree of incorporation of magnetic material during synthesis of the composite.

Magnetite has  $\text{O}_2^-$  ions coordinated with  $\text{Fe}^{2+}$  and  $\text{Fe}^{3+}$  ions in octahedral interstices and  $\text{Fe}^{3+}$  in tetrahedral interstices. Considering that  $\text{Fe}^{3+}$  ions are present in both interstices, these ions do not have a resulting magnetic moment, and the saturation magnetization is provoked by  $\text{Fe}^{2+}$  ions at octahedral interfaces (Figure 1c). The presence of  $\text{Fe}^{2+}$  ions in the spinel of octahedral sites makes these oxides promising catalysts of the Fenton process. Maghemite has a structure like a magnetite but only contains  $\text{Fe}^{3+}$ . Goethite has an orthorhombic structure, with  $\text{Fe}^{3+}$  ions coordinated with  $\text{O}^{2-}$  and  $\text{OH}^-$  ions<sup>[19,20]</sup>. This magnetic material can act in two ways in Fenton catalysis: (i)  $\text{Fe}^{2+}$  ions in magnetite domains can act directly on the decomposition of  $\text{H}_2\text{O}_2$ ; or (ii)  $\text{Fe}^{3+}$  ions in maghemite and goethite domains can coordinate with  $\text{H}_2\text{O}_2$  molecules, generating  $[\text{Fe}(\text{III})\text{OOH}]^{2+}$  ions, which undergo decomposition, generating OH and OOH radicals (Figure 2)<sup>[8,21]</sup>.

Thus, considering that the  $\text{Fe}^{2+}$  and  $\text{Fe}^{3+}$  ions present in magnetic material can act as catalysts of Fenton reactions, we conducted studies of MO degradation in the presence of magnetic microspheres by varying the pH of the medium, the mass of this composite, and concentration of  $\text{H}_2\text{O}_2$ .

### 3.1 Variation of the concentration of $\text{H}_2\text{O}_2$

The following reaction conditions were employed to study the effect of  $\text{H}_2\text{O}_2$  concentration on MO degradation: 5 ppm dye, 1% composite, 10 minutes of contact, pH 3, and varying concentrations of hydrogen peroxide (1.0, 5.0, 20, and 50 ppm). The first results are shown in Figure 3a. We expected the increase in  $\text{H}_2\text{O}_2$  concentration to be associated with a higher content of reactive radicals, consequently increasing the dye degradation rate. The color removal rate varied little with alteration of the  $\text{H}_2\text{O}_2$  concentration, indicating that the reaction equilibrium was achieved. To confirm this observation, a second experiment was carried out using peroxide concentrations of 10 and 20 ppm, 5% composite, and varying the contact time between the composite and solution. The data are shown in Figure 3b. Similar removal rates were found employing 10 ppm or 20 ppm of  $\text{H}_2\text{O}_2$  in the reaction time range of 0 to 30 minutes. The increase of  $\text{H}_2\text{O}_2$  resulted from scavenging excess hydroxyl radicals, generating water and other byproducts with lower oxidation potential ( $\cdot\text{HO}_2$  and  $\cdot\text{-O}_2$ ), which did not contribute to reducing the dye removal<sup>[1,11]</sup>. Quadrado et al.<sup>[11]</sup> studied the influence of peroxide concentration on the action of the heterogeneous Fenton process for the decomposition of OM dye. When the peroxide concentration was increased from  $5\text{ mmol L}^{-1}$  to  $20\text{ mmol L}^{-1}$ , the dye removal speed was slower, i.e., in 20 minutes, the removal rate reached 90% with  $5\text{ mmol L}^{-1}$   $\text{H}_2\text{O}_2$  and only 40% with  $20\text{ mmol L}^{-1}$   $\text{H}_2\text{O}_2$  in the same period. According to these authors, at high concentrations of  $\text{H}_2\text{O}_2$ , the generation of radicals ( $\cdot\text{OH}$ ) is not selective, and the  $\text{H}_2\text{O}_2$  molecules can be

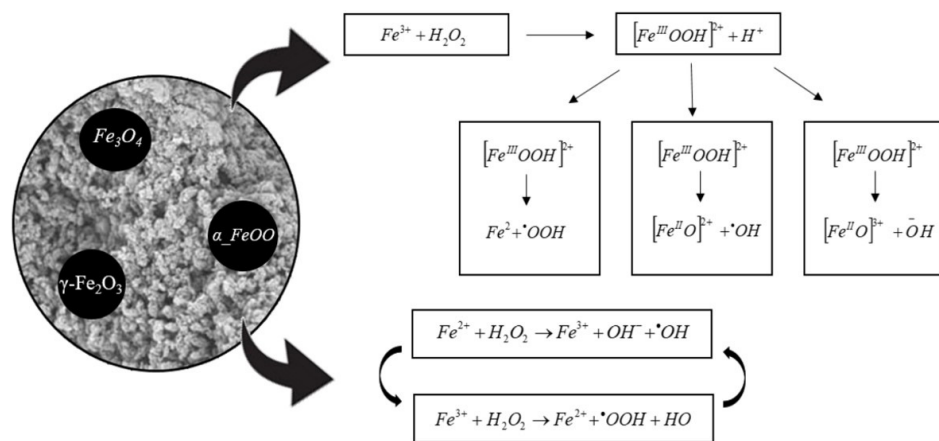


**Figure 2.** Principal reactions involving ferrous ions in magnetite, maghemite and goethite domains. Based on the works of Panda et al.<sup>[14]</sup> and Wan et al.<sup>[21]</sup>.

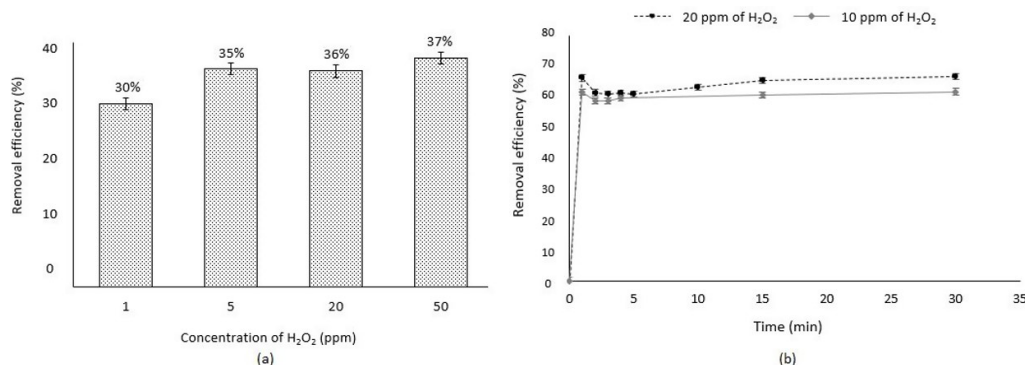


**Figure 3.** (a) Effect of H<sub>2</sub>O<sub>2</sub> content on degradation of MO (a: H<sub>2</sub>O<sub>2</sub> content: 1-50 ppm, pH: 3, MO: 5 ppm, composite: 1%, time: 10 minutes), (b: H<sub>2</sub>O<sub>2</sub> content: 10 or 20 ppm, pH: 3, MO: 5 ppm, composite: 5%, time: 1-30 minutes).

decomposed into water and oxygen. In addition, the radical ( $\cdot\text{OH}$ ) generated can be consumed by the H<sub>2</sub>O<sub>2</sub> itself, resulting in hydroperoxyl radicals ( $\cdot\text{OOH}$ ). These radicals ( $\cdot\text{OOH}$ ) have less oxidizing power and can also eliminate radicals ( $\cdot\text{OH}$ ), decreasing the dye removal efficiency. Shi et al.<sup>[22]</sup> reported similar observations. They studied the influence of H<sub>2</sub>O<sub>2</sub> concentration in a heterogeneous Fenton process for dye decomposition. Their results showed that the dye removal rate increased with the increase of H<sub>2</sub>O<sub>2</sub> concentration, limited to an optimal concentration value, from which there was an excess of H<sub>2</sub>O<sub>2</sub> and consequently decreased formation of radicals ( $\cdot\text{OH}$ ).

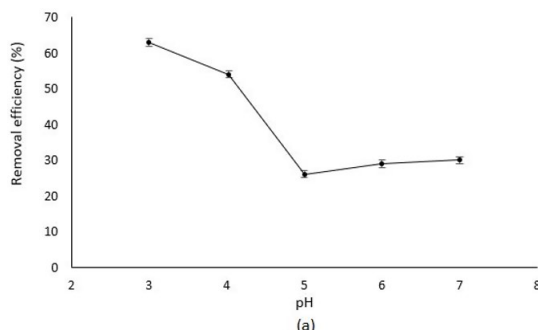
### 3.2 Variation of pH of the medium

Dye removal was investigated by employing a pH range between 3 and 7 and keeping constant all other parameters: 5 ppm of MO, 5 ppm of H<sub>2</sub>O<sub>2</sub>, 5% composite, and 10 minutes of reaction (Figure 4a). The highest color removal (63%) was achieved at pH 3.0, and there was a decrease in dye decomposition with rising pH (above pH 5.0, the dye removal rate was only 30%).

The increasing dye discoloration at lower pH suggests that Fe<sup>2+</sup> and Fe<sup>3+</sup> ions are released in the medium from the composite, i.e., magnetic microspheres may act as

“demand-release homogeneous Fenton catalysts”. Chu and colleagues<sup>[23]</sup> observed dependence between the removal rate of dyes in a Fenton process catalyzed by magnetic biochar and the pH level, which was related to the reaction conditions. According to these authors, the increase of the dye removal with decreasing pH can be explained by the decreasing iron solubility and oxidation potential of peroxide radicals, in contrast to the self-decomposition of H<sub>2</sub>O<sub>2</sub> to H<sub>2</sub>O and O<sub>2</sub> at higher pH. On the other hand, Vu and colleagues<sup>[24]</sup> reported that at pH lower than 2.5, the efficiency of the Fenton reaction decreases significantly due to the formation of H<sub>3</sub>O<sup>+</sup> ions and complexes such as [Fe(H<sub>2</sub>O)<sup>6</sup>]<sup>2+</sup> and Fe(H<sub>2</sub>O)<sup>6</sup><sup>3+</sup>, along with the “scavenging effect” of hydroxyl radicals by excessive content of H<sup>+</sup> ions (OH<sup>-</sup> + H<sup>+</sup> + e  $\rightarrow$  H<sub>2</sub>O).

The evaluation of the supernatant containing the reagents H<sub>2</sub>O<sub>2</sub>, dye, and 5 or 20% of composite by Inductively Coupled Plasma Optical Emission Spectrometry (ICP-OES) (Thermo-Scientific, Model ICAP 6300 DUO) revealed concentrations of 0.23±0.01 and 0.33±0.01 mg L<sup>-1</sup> of Fe metal in this medium. Considering that the content of Fe metal introduced during the polymerization was 83 mg g<sup>-1</sup> of polymer, we can affirm that the magnetic microspheres did not act as “demand-release homogeneous Fenton catalysts”.



(a)

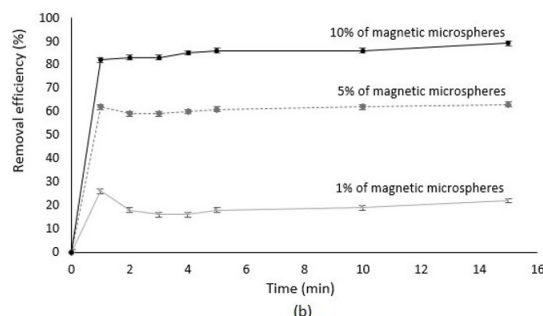


**Figure 4.** (a) Effect of pH on MO degradation. Experimental conditions: pH 3-7.3, 5 ppm of MO, 5 ppm of  $\text{H}_2\text{O}_2$ , 5% of composite, and 10 minutes of reaction; (b) Effect of catalyst on the degradation of MO in the function of time. Experimental conditions: pH 3, 5 ppm of MO, 20 ppm of  $\text{H}_2\text{O}_2$ , 5% of composite, contact time range from 0-30 minutes.

It is also possible to suppose that some of the dye molecules were adsorbed by magnetic microspheres, and this adsorption was more favorable in acid media. The acid dissociation constant ( $\text{pK}_a$ ) for methyl orange is 3.46. Thus, at pH 3 the dye molecules are in neutral form, while above this pH, these molecules are in salt form, presenting  $\text{SO}_3^- \text{Na}^+$  groups<sup>[1]</sup>. Probably the adsorption of these molecules was favored in their neutral form due to the formation of hydrogen bonds involving the  $\text{SO}_3^-$  groups (not dissociated) of the dye and iron oxide domains of the magnetic material.

### 3.3 Variation of the magnetic microsphere mass and contact time

Here we used 10 ppm of hydrogen peroxide, 5 ppm of MO, different composite contents (1%, 5% and 10% (w/v)) and contact times (1, 2, 3, 4, 5, 10 and 15 minutes). The data shown in Figure 4b indicate that increasing composite mass resulted in rinsing dye removal efficiency. The highest removal rate (close to 90%) was achieved using 10% w/v of the composite material. This can be explained considering that the increase of composite contributed to increasing the concentration of  $\text{Fe}^{2+}$  and  $\text{Fe}^{3+}$  ions (consequently favoring the Fenton process) and increasing the absorbance of this dye from the medium. Arshadi and colleagues<sup>[1]</sup> reported that a large excess of catalyst could have two consequences: self-scavenging of OH radicals by ferrous ions, resulting in a reduction of dye decomposition; or aggregation of the particles due to increased collision between them, resulting in lower total surface area and greater diffusion path length, in turn reducing the adsorption capacity.

The dye removal was most significant in the first minute of the reaction, achieving a reduction of more than 80% by using 10% composite because equilibrium was reached after one minute. This result also can indicate that MO degradation is related not only to the generation of reactive radicals involving  $\text{Fe}^{2+}$  and  $\text{Fe}^{3+}$  ions present in the magnetic material, but also to release of these ions from the composite. It is possible to suppose that some of the dye molecules are adsorbed by magnetic polymeric particles. In the first stage of adsorption, many active sites are available to dye molecules, so the reduction of available sites combined with repulsion between these dye molecules surrounding the particles and the molecules on the surface of the particles

might have resulted in more negligible adsorption after the first minute of contact<sup>[25]</sup>.

### 3.4 Study of adsorption capacity

For these experiments, 10 mL of MO solution (5 ppm) was put in contact with the different concentrations of composite (5%, 10% or 20% (w/v)) for 10 minutes. After this period, the absorbance in each flask was analyzed. Then, 10 ppm of  $\text{H}_2\text{O}_2$  was added to each flask, and after 10 minutes of contact, the absorbance was reread. The results obtained are shown in Figure 5.

According to Figure 5, there was a significant increase in the dye removal rate with more extended contact of the dye with the composite, in the absence of  $\text{H}_2\text{O}_2$ . The variation in composite mass was accompanied by increasing color removal. It can be inferred that the composite had high MO adsorption capacity and that this characteristic strongly influenced the color removal rate in all stages of this study. After the addition of  $\text{H}_2\text{O}_2$  in the medium, there was a further increase in the removal rate. The “total color removals,” as identified in the legend of Figure 5, were 55%, 66%, and 56% for composite concentrations of 5%, 10%, and 20%, respectively. Based on these results, it is possible to suppose that the total removal data represent the sum of the adsorption effect and the color removal due to oxidation of the MO by the  $\text{Fe}^{2+}$  and  $\text{Fe}^{3+}$  ions present in the magnetic material of the polymer matrix. In other words, the analysis of these data allows us to assume that the adsorption and oxidation mechanisms act together for the variation of MO removal in a heterogeneous Fenton process with the composite as a catalyst. The dye removal rate obtained via the oxidative process accompanied the dye removal by adsorption when employing 5 and 10% particles. Still, when 15% composite was used, the removal rate due to the Fenton reaction was lower than the removal due to adsorption, probably because of self-scavenging of OH radicals by ferrous ions, resulting in a reduction of dye decomposition.

Xu et al. (2018)<sup>[10]</sup> studied the degradation of MO by applying a heterogeneous Fenton process using magnetite and a composite of reduced graphene oxide as catalysts for dye decomposition. The results showed that the composite used had high dye adsorption capacity, reaching 57% removal (by adsorption) after 30 minutes of contact. A synergistic effect

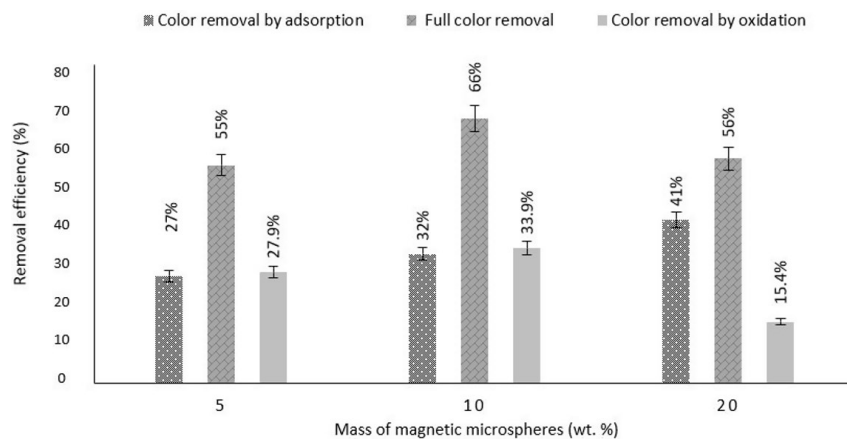


**Figure 5.** Color removal of MO due to adsorption and oxidation by Fenton processes. Experimental conditions: pH 3, 5 ppm of MO, 20 ppm of  $\text{H}_2\text{O}_2$ , 5%-20% wt.% of composite, contact time range from 0-20 minutes.

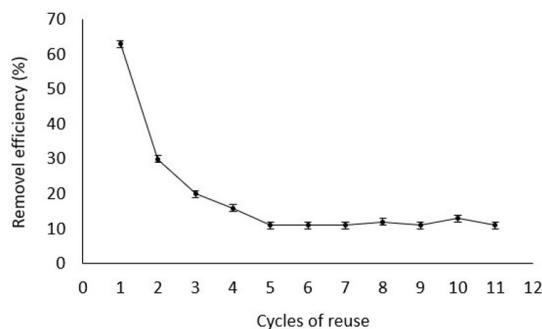


**Figure 6.** Study of reuse of composite particles for MO removal. Experimental conditions: pH 3, 5 ppm of MO, 10 ppm of  $\text{H}_2\text{O}_2$ , 5% of composite, contact time of 5 minutes.

was observed in the Fenton-type reaction and adsorption governing the degradation of the dye in the studied system. Because of this synergistic effect, the removal achieved was 94%.

### 3.5 Reuse assessment

To evaluate the possibility of reusing the composite for degradation of MO, decomposition tests were carried out by using 5% (w/v) of composite, 10 ppm of  $\text{H}_2\text{O}_2$ , 5 ppm of dye, pH 3.0, and 5 minutes of contact until there was no significant variation in the absorbance readings. This study determined the decomposition after each cycle by analyzing the absorbance at 500 nm. The efficiency of the composite was evaluated in a sequence of 11 reuse cycles (Figure 6). As shown in Figure 6, the initial removal rate was 63%. During the catalyst reuse cycles, there was a gradual decline in this value until the fifth cycle, from 63% to 10%, clearly indicating a loss of functionality of the composite as a catalyst and its adsorption capacity. From the fifth reuse cycle onward, the removal rate was close to 10%, and no significant variations were observed until the 11th cycle, indicating that the maximum number of economically feasible cycles is four. The reuse of catalysts has been investigated by several researchers<sup>[10,11,23,26]</sup>. Shao and Chen<sup>[26]</sup> studied the reuse of the catalyst and obtained high removal rates

with slight variation until the third cycle. Quadrado and Fajardo<sup>[11]</sup> evaluated the reuse of the catalyst in the Fenton process for the decomposition of dyes. They observed that the catalyst-maintained color removal efficiency above 98% during five reuse cycles.

## 4. Conclusions

In the present study, magnetic PMMA microspheres prepared by aqueous suspension polymerization were evaluated as catalysts for the decomposition of MO through a heterogeneous Fenton process. These microspheres showed a larger size distribution of the particles (20–104  $\mu\text{m}$ ), specific surface area of  $48 \text{ m}^2 \text{ g}^{-1}$ , and pore volume of  $0.35 \text{ m}^2 \text{ g}^{-1}$ . Data from XRD showed the presence of iron oxides in this material and that the magnetic material was preserved during polymerization. These data along with data of FT-IR showed that both monomers (MMA and crosslinking agent DVB) were also included in microspheres. Mossbauer data showed that these microspheres contained a mixture of minerals with magnetic behavior (31% magnetite and 21% maghemite). The observation of saturation magnetization and remaining magnetization of 4.76 and 0.21, respectively, showed that this material had superparamagnetic behavior. There was no significant variation in the color removal rate with variation in the concentration of  $\text{H}_2\text{O}_2$  (1–50 ppm), around 30% by employing 1% of composite and around 60% by employing 5% composite. Still, color removal increased with a higher composite mass and was most pronounced in the first minute of contact between MO and composite, around 80% by employing 10% microspheres. The need for pH control in this system proved to be a very restrictive condition since the rates of color removal were much lower with pH above 3. The adsorption studies of the dye by the composite, carried out in the absence of  $\text{H}_2\text{O}_2$ , confirmed the adsorption of the MO dye by this material. This characteristic strongly influenced the color removal rate at all stages of this study. The reuse of the composite was evaluated for color removal in 11 reuse cycles, and the results indicated that from the first to the fifth reuse cycle, the color removal rate declined to about 50%.

The results also indicated that the adsorption and oxidation mechanisms vary the MO dye removal rate in this heterogeneous Fenton process, with the composite as a catalyst. The results in this work suggest that the composite acts both in the dye adsorption and in the decomposition of H<sub>2</sub>O<sub>2</sub>. We achieved a maximum color removal rate of 90% using 10% (w/v) of composite, 10 ppm of peroxide, pH 3.0, 5 ppm of dye, and a contact time of 10 minutes. The composite can be applied to aid in treating effluents contaminated with dyes. However, further studies are necessary to overcome the restriction related to the pH of this material and to extend useful life.

## 5. Author's Contribution

- **Conceptualization** – Luciana da Cunha Costa; Mônica Regina da Costa Marques.
- **Data curation** – NA.
- **Formal analysis** – NA.
- **Funding acquisition** – Luciana da Cunha Costa; Mônica Regina da Costa Marques.
- **Investigation** – Alan Kardec Silva; Jacira Aparecida Castanharo.
- **Methodology** – Alan Kardec Silva; Jacira Aparecida Castanharo.
- **Project administration** – NA.
- **Resources** – NA.
- **Software** – NA.
- **Supervision** – Luciana da Cunha Costa; Mônica Regina da Costa Marques.
- **Validation** – NA.
- **Visualization** – NA.
- **Writing – original draft** – Alan Kardec Silva; Ezaine Cristina Corrêa Torquato.
- **Writing – review & editing** – Luciana da Cunha Costa; Jacira Aparecida Castanharo; Marcos Antonio da Silva Costa; Mônica Regina da Costa Marques.

## 6. Acknowledgements

We thank the Rio de Janeiro State Research Foundation (FAPERJ) for financial support.

## 7. References

1. Arshadi, M., Abdolmaleki, M. K., Mousavinia, F., Khalafinezhad, A., Firouzabadi, H., & Gil, A. (2016). Degradation of methyl orange by heterogeneous Fenton-like oxidation on a nano-organometallic compound in the presence of multi-walled carbon nanotubes. *Chemical Engineering Research & Design*, 112, 113-121. <http://dx.doi.org/10.1016/j.cherd.2016.05.028>.
2. Alansi, A. M., Al-Qunaibit, M., Alade, I. O., Qahtan, T. F., & Saleh, T. A. (2018). Visible-light responsive BiOBr nanoparticles loaded on reduced graphene oxide for the photocatalytic degradation of dye. *Journal of Molecular Liquids*, 253, 297-304. <http://dx.doi.org/10.1016/j.molliq.2018.01.034>.
3. Tunç, S., Gürkan, T., & Duman, O. (2012). On-line spectrophotometric method for the determination of optimum operation parameters on the decolorization of Acid Red 66 and Direct Blue 71 from aqueous solution by Fenton process. *Chemical Engineering Journal*, 181-182, 431-442. <http://dx.doi.org/10.1016/j.cej.2011.11.109>.
4. Liu, Y., Zhang, G., Chong, S., Zhang, N., Chang, H., Huang, T., & Fang, S. (2017). NiFe(C<sub>2</sub>O<sub>4</sub>)<sub>x</sub> as a heterogeneous Fenton catalyst for the removal of methyl orange. *Journal of Environmental Management*, 192, 150-155. <http://dx.doi.org/10.1016/j.jenvman.2017.01.064>. PMid:28160642.
5. Ferroudj, N., Beaumier, P., Davidson, A., & Abramson, S. (2021). Fe<sup>3+</sup>-doped ordered mesoporous γ-Fe<sub>2</sub>O<sub>3</sub>/SiO<sub>2</sub> microspheres as a highly efficient magnetically separable heterogeneous Fenton catalyst. *Microporous and Mesoporous Materials*, 326, 111373. <http://dx.doi.org/10.1016/j.micromeso.2021.111373>.
6. Castanharo, J. A., Ferreira, I. L. M., Costa, M. A. S., Silva, M. R., Costa, G. M., & Oliveira, M. G. (2015). Magnetic microspheres based on poly(divinylbenzene-co-methyl methacrylate) obtained by suspension polymerization. *Polímeros: Ciência e Tecnologia*, 25(2), 192-199. <http://dx.doi.org/10.1590/0104-1428.1666>.
7. Castanharo, J. A., Ferreira, I. L. M., Silva, M. R., & Costa, M. A. S. (2018). Core-shell magnetic particles obtained by seeded suspension polymerization of acrylic monomers. *Polímeros: Ciência e Tecnologia*, 28(5), 460-467. <http://dx.doi.org/10.1590/0104-1428.10517>.
8. Jaiswal, K. K., Manikandan, D., Murugan, R., & Ramaswamy, A. P. (2018). Microwave-assisted rapid synthesis of Fe<sub>3</sub>O<sub>4</sub>/Poly(styrene-divinylbenzene-acrylic acid) polymeric magnetic composites and investigation of their structural and magnetic properties. *European Polymer Journal*, 98, 177-190. <http://dx.doi.org/10.1016/j.eurpolymj.2017.11.005>.
9. Abdullah, N., Tajuddin, M. H., & Yusof, N. (2018). Carbon-based polymer nanocomposites for dye and pigment removal. In A. F. Ismail & P. S. Goh (Eds.), *Carbon-based polymer nanocomposites for environmental and energy applications* (pp. 305-329). India: Elsevier. <http://dx.doi.org/10.1016/B978-0-12-813574-7.00013-7>.
10. Xu, H., Li, B., Shi, T., Wang, Y., & Komarneni, S. (2018). Nanoparticles of magnetite anchored onto few-layer graphene: a highly efficient Fenton-like nanocomposite catalyst. *Journal of Colloid and Interface Science*, 532, 161-170. <http://dx.doi.org/10.1016/j.jcis.2018.07.128>. PMid:30081262.
11. Quadrado, R. F. N., & Fajardo, A. R. (2017). Fast decolorization of azo methyl orange via heterogeneous Fenton and Fenton-like reactions using alginate-Fe<sup>2+</sup>/Fe<sup>3+</sup> films as catalysts. *Carbohydrate Polymers*, 177, 443-450. <http://dx.doi.org/10.1016/j.carbpol.2017.08.083>. PMid:28962790.
12. Gao, Y., Zhang, J., Liang, J., Yuan, D., & Zhao, W. (2022). Research progress of poly(methyl methacrylate) microspheres: preparation, functionalization and application. *European Polymer Journal*, 175, 111379. <http://dx.doi.org/10.1016/j.eurpolymj.2022.111379>.
13. Shan, J., Wang, L., Yu, H.-J., Tai, Y., & Akram, M. (2015). Synthesis and characterization of magnetic porous Fe<sub>3</sub>O<sub>4</sub>/poly(methylmethacrylate-co-divinylbenzene) microspheres and their use in removal of Rhodamine B. *Journal of Zhejiang University. Science A*, 16(8), 669-679. <http://dx.doi.org/10.1631/jzus.A1500096>.
14. Panda, N., Sahoo, H., & Mohapatra, S. (2011). Decolorization of methyl orange using Fenton-like mesoporous Fe<sub>2</sub>O<sub>3</sub>-SiO<sub>2</sub> composite. *Journal of Hazardous Materials*, 185(1), 359-365. <http://dx.doi.org/10.1016/j.jhazmat.2010.09.042>. PMid:20934248.

15. Chen, Z., Jin, X., Chen, Z., Megharaj, M., & Naidu, R. (2011). Removal of methyl orange from aqueous solution using bentonite-supported nanoscale zero-valent iron. *Journal of Colloid and Interface Science*, 363(2), 601-607. <http://dx.doi.org/10.1016/j.jcis.2011.07.057>. PMID:21864843.
16. Silverstein, R. M., Webster, F. X., & Kiemle, D. J. (2005). *Spectrometric identification of organic compounds*. New York: John Wiley & Sons.
17. Polikarpov, M., Cherepanov, V., Chuev, M., Shishkov, S., & Yakimov, S. (2010). Mössbauer spectra of hematite and magnetite nanoparticles in polymer composites. *Journal of Physics: Conference Series*, 217, 012114. <http://dx.doi.org/10.1088/1742-6596/217/1/012114>.
18. Thakur, M., De, K., Giri, S., Si, S., Kotal, A., & Mandal, T. K. (2006). Interparticle interaction and size effect in polymer coated magnetic nanoparticles. *Journal of Physics Condensed Matter*, 18(39), 9093-9104. <http://dx.doi.org/10.1088/0953-8984/18/39/035>.
19. Oliveira, L. C. A., Fabris, J. D., & Pereira, M. C. (2013). Iron oxides and their applications in catalytic processes: a review. *Química Nova*, 36(1), 123-130. <http://dx.doi.org/10.1590/S0100-40422013000100022>.
20. Freitas, N. S., Alzamora, M., Sanchez, D. R., Licea, Y. E., Senra, J. D., & Carvalho, N. M. F. (2021). Green palladium nanoparticles prepared with glycerol and supported on maghemite for dye removal application. *Journal of Environmental Chemical Engineering*, 9(1), 104856. <http://dx.doi.org/10.1016/j.jece.2020.104856>.
21. Wan, D., Li, W., Wang, G., Lu, L., & Wei, X. (2017). Degradation of p-Nitrophenol using magnetic Fe<sup>0</sup>/Fe<sub>3</sub>O<sub>4</sub>/Coke composite as a heterogeneous Fenton-like catalyst. *The Science of the Total Environment*, 574, 1326-1334. <http://dx.doi.org/10.1016/j.scitotenv.2016.08.042>. PMID:27519319.
22. Shi, X., Tian, A., You, J., Yang, H., Wang, Y., & Xue, X. (2018). Degradation of organic dyes by a new heterogeneous Fenton reagent - Fe<sub>2</sub>GeS<sub>4</sub> nanoparticle. *Journal of Hazardous Materials*, 353, 182-189. <http://dx.doi.org/10.1016/j.jhazmat.2018.04.018>. PMID:29674093.
23. Chu, J., Kang, J., Park, S., & Lee, C. (2020). Application of magnetic biochar derived from food waste in heterogeneous sono-Fenton-like process for removal of organic dyes from aqueous solution. *Journal of Water Process Engineering*, 37, 101455. <http://dx.doi.org/10.1016/j.jwpe.2020.101455>.
24. Vu, A.-T., Xuan, T. N., & Lee, C.-H. (2019). Preparation of mesoporous Fe<sub>2</sub>O<sub>3</sub>·SiO<sub>2</sub> composite from rice husk as an efficient heterogeneous Fenton-like catalyst for degradation of organic dyes. *Journal of Water Process Engineering*, 28, 169-180. <http://dx.doi.org/10.1016/j.jwpe.2019.01.019>.
25. Wołowicz, A., & Hubicki, Z. (2010). Effect of matrix and structure types of ion exchangers on palladium(II) sorption from acidic medium. *Chemical Engineering Journal*, 160(2), 660-670. <http://dx.doi.org/10.1016/j.cej.2010.04.009>.
26. Shao, Y., & Chen, H. (2018). Heterogeneous Fenton oxidation of phenol in fixed-bed reactor using Fe nanoparticles embedded within ordered mesoporous carbons. *Chemical Engineering Research & Design*, 132, 57-68. <http://dx.doi.org/10.1016/j.cherd.2017.12.039>.

*Received: Apr. 13, 2022**Revised: July 19, 2022**Accepted: July 22, 2022*

## **Supplementary Material**

Supplementary material accompanies this paper.

**Figure S1:** Publications on heterogeneous Fenton and magnetic composites over the years. (Database ScienceDirect, accessed in July 2022, keywords: heterogeneous Fenton and magnetic composites)

This material is available as part of the online article from <https://doi.org/10.1590/0104-1428.20220029>